Science of the Total Environment 850 (2022) 157971

Contents lists available at ScienceDirect

Science of the Total Environment

journal homepage: www.elsevier.com/locate/scitotenv

The strontium isotope fingerprint of phosphate rocks mining

Avner Vengosh [a,*], Zhen Wang [a], Gordon Williams [a], Robert Hill [a], Rachel M. Coyte [b], Gary S. Dwyer [a]

[a] Nicholas School of the Environment, Duke University, Durham, NC 27708, USA
[b] School of Earth Sciences, The Ohio State University, Columbus, OH 43210, USA

HIGHLIGHTS

- Phosphate wastewater contains elevated levels of meta(loid)s.
- The environmental impacts of phosphate mining operation are not always clear.
- Debate over the source of contamination of saline groundwater in the Negev, Israel.
- Strontium isotopes is used to delineate the effects of phosphate mining.
- The strontium isotope data of the saline groundwater rule out contamination from phosphate wastewater.

GRAPHICAL ABSTRACT

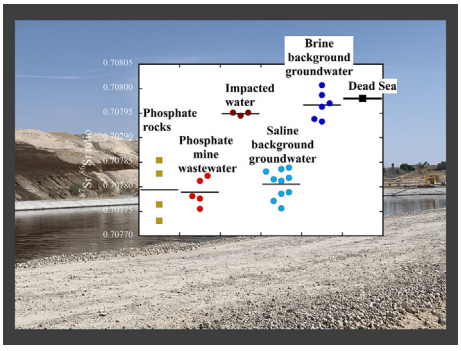

ARTICLE INFO

Editor: Daniel Alessi

Keywords:
Phosphate mining
Water contamination
Metals
Isotope tracers

ABSTRACT

High concentrations of metal(loid)s in phosphate rocks and wastewater associated with phosphate mining and fertilizer production operations pose potential contamination risks to water resources. Here, we propose using Sr isotopes as a tracer to determine possible water quality impacts induced from phosphate mining and fertilizers production. We utilized a regional case study in the northeastern Negev in Israel, where salinization of groundwater and a spring have been attributed to historic leaking and contamination from an upstream phosphate mining wastewater. This study presents a comprehensive dataset of major and trace elements, combined with Sr isotope analyses of the Rotem phosphate rocks, local aquifer carbonate rocks, wastewater from phosphate operation in Mishor Rotem Industries, saline groundwater suspected to be impacted by Rotem mining activities, and two types of background groundwater from the local Judea Group aquifer. The results of this study indicate that trace elements that are enriched in phosphate wastewater were ubiquitously present in the regional and non-contaminated groundwater at the same levels as detected in the impacted waters, and thus cannot be explicitly linked to the phosphate wastewater. The $^{87}Sr/^{86}Sr$ ratios of phosphate rocks ($0.707794 \pm 5 \times 10^{-5}$) from Mishor Rotem Industries were identical to that of associated wastewater ($0.707789 \pm 3 \times 10^{-5}$), indicating that the Sr isotopic fingerprint of phosphate rocks is preserved in its wastewater. The $^{87}Sr/^{86}Sr$ ($0.707949 \pm 3 \times 10^{-6}$) of the impacted saline groundwater were significantly different from those of the Rotem wastewater and the background saline groundwater, excluding phosphate mining effluents as the major source for contamination of the aquifer. Instead, the $^{87}Sr/^{86}Sr$ ratio of the impacted water was similar to the composition of brines from the Dead Sea, which suggests that the salinization was derived primarily from industrial Dead Sea effluents with distinctive Sr isotope and geochemical fingerprints.

1. Introduction

Phosphorus is one of the primary nutrients essential for plant growth and crop production and thus its availability is critical for sustainable

* Corresponding author.
E-mail address: vengosh@duke.edu (A. Vengosh).

http://dx.doi.org/10.1016/j.scitotenv.2022.157971
Received 3 July 2022; Received in revised form 6 August 2022; Accepted 7 August 2022
Available online 11 August 2022
0048-9697/© 2022 Elsevier B.V. All rights reserved.

agricultural development and food security. Phosphate fertilizers are typically produced from acid dissolution of phosphate rocks by sulfuric acid to generate single super phosphate (SSP, 16–21 % P_2O_5) and/or phosphoric acid, which is also used to generate triple super phosphate (TSP, 43–48 % P_2O_5). As part of fertilizer production, phosphogypsum is generated as a byproduct (World Bank Group, 2007). Previous studies have reported elevated levels of U, Cd, and other metal(loid)s in phosphate rocks (Schnug and Haneklaus, 2015; Shang et al., 2021; Sun et al., 2020; Nio-Savala et al., 2019; Bigalke et al., 2017; Gill and Shiloni, 1995; Jiao et al., 2012; Li et al., 2020; Menzel, 1968; Zhuang and McBride, 2013). During phosphate mining and fertilizer production, phosphorus (P) in addition to metal(loid)s from phosphate rocks are mobilized into the low-pH wastewater and byproducts, posing environmental risks to the surrounding areas (Cotter-Howells and Caporn, 1996; Macías et al., 2017; Reta et al., 2018; Taha et al., 2021). Several studies have shown metal and radionuclide contamination in the acidic mine wastewater and phosphogypsum byproduct such as in Jordan (Al-Hwaiti et al., 2018), Morocco (Belgada et al., 2021; Taha et al., 2021), Tunisia (Mabrouk et al., 2020; Khelifi et al., 2022), Syria (Othman and Al-Masri, 2007), Turkey (Aydin et al., 2010), Pakistan (Sabiha-Javied et al., 2009), Croatia (Bituh et al., 2009), Spain (Pérez-López et al., 2010), Togo (Gnandi et al., 2006), and the U.S. (Rutherford et al., 1994; Burnett and Elzerman, 2001; Hamilton et al., 2002; Myers, 2013).

While dissolution of phosphate rocks and the formation of acidic and highly saline wastewater for fertilizers production has been recognized as one of the potential environmental risks of phosphate mining (Reta et al., 2018), the ability to establish a direct link between water quality degradation and phosphate mining is not always trivial. Phosphorus that is present in water as the orthophosphate ion (PO_4^{3-}) is highly reactive and is commonly retained by the aquifer rocks through adsorption onto clay minerals (Holtan et al., 1988). The concentrations of metal(loid)s in groundwater resources can also be affected by variations of their speciation that are controlled by multiple geochemical factors (e.g., salinity, pH, oxidation-reduction). Therefore, the abundance of metal(loid)s in the phosphate wastewater could also be modified through water-rock interactions along the effluent and/or groundwater flow paths, thereby masking the original wastewater chemical composition. For example, the high acidity of the phosphate wastewater infiltrating into the subsurface could dissolve aquifer rocks, causing an increase in pH and consequently, a retention of metal(loid)s from the industrial wastewater, resulting in low concentrations of metal(loid)s in contaminated groundwater (Arad and Halicz, 1994). Furthermore, in some cases other industrial sources can cause contamination, in addition to the possible presence of naturally occurring (geogenic) contaminants in the aquifers that can also affect the water quality.

To address these limitations, we propose using strontium (Sr) isotopes as a tracer for phosphate mining impacts on water resources. Strontium is an alkaline-earth metal that occurs mostly as a cation (Sr^{2+}) that is highly soluble in natural water. Numerous studies have shown the advantages of using Sr isotopes as a geochemical tracer that can preserve the original isotope fingerprint of the contamination sources with minimal modification induced from secondary water-rock interactions. While phosphorus and metals from the phosphate wastewater can be retained through adsorption and co-precipitation on clay minerals and oxides in the aquifer, the Sr isotopes ratio in the water is not affected by Sr adsorption, and thus the original Sr isotope ratio of the contamination source is preserved (McNutt, 2000; Capo et al., 1998; Cook and Herczeg, 2000; Harkness et al., 2017; Ruhl et al., 2014; Vengosh et al., 2016; Warner et al., 2014). This study aims to test the utility of Sr isotopes as a potential tracer for detecting the impact of phosphate mining and associated wastewater on the environment though investigating different water sources associated with phosphate mining and wastewater in the northeastern Negev, Israel (Fig. 1). We present a unique dataset that includes phosphate rocks from the Rotem phosphate field, associated wastewaters from a phosphate fertilizer factory in Mishor Rotem Industries (MRI), downstream saline groundwater that was previously suggested to be contaminated from the phosphate mine effluents (Burg and Guttman, 2019), and background groundwater and aquifer rocks of the Judea Group aquifer in northeastern Negev, Israel. While Sr isotope geochemistry has been employed for tracing groundwater contamination in numerous cases and has been analyzed in phosphate rocks (Sattouf, 2007; Sattouf et al., 2007, 2008; Soudry et al., 2006), as far as we are aware, this is the first time that it has been utilized to delineate the possible contamination of groundwater by effluents from phosphate mining and the use of Sr isotopes as a novel geochemical tracer to delineate the impact of phosphate mining on the environment. Given the high concentrations of Sr in the phosphate wastewater (up to 155 mg/L), compared to the background saline groundwater (4–7 mg/L), we hypothesize that the Sr isotope fingerprint of the phosphate wastewater would be preserved upon groundwater contamination. In addition to evaluating the Sr isotope systematics as a potential tracer for phosphate mine wastewater in the environment, this study presents a comprehensive dataset of trace elements abundances in phosphate rocks, phosphate mining wastewater, and different groundwater resources from the Northeastern Negev of Israel.

2. Background and methods

2.1. Background

The phosphate rocks of Rotem field (Fig. 1) are part of the Campanian Mishash Formation in the northeastern Negev, Israel (Soudry, 1992; Soudry et al., 2006, 2013). Since the early-1970's, phosphate rocks in the Rotem field in MRI have been mined to generate phosphoric acid, fertilizers, phosphogysum byproduct, and wastewater. During the early stages of operations, industrial wastewaters from phosphate mining, combined with other wastewaters such as Dead Sea Water Type (DSWT) from the nearby magnesium oxide industry (Periclas) have been disposed to several open reservoirs in MRI (Fig. 1). Previous studies have suggested that leaking of these reservoirs in MRI has caused the infiltration of industrial wastewaters to the subsurface (Burg and Naor, 2000; Arad and Halicz, 1994) and caused the contamination of downstream groundwater from the Cenomanian part of the Judea Group aquifer. It has been suggested that the contaminated groundwater has migrated in the Judea Group aquifer (Zafit Formation) towards well Efe 13a (Fig. 1), following the hydrogeological structure in the aquifer (Burg and Gavrieli, 2013; Burg and Guttman, 2019; Burg and Naor, 2000). These studies have suggested that the downgradient flow of the contaminated groundwater had caused the increase of the salinity in Efe 13a and Ein Bokek, located further downstream towards the Dead Sea Rift Valley emerging as a natural outlet of the aquifer (Fig. 1) (Burg and Gavrieli, 2013; Burg and Guttman, 2019; Burg and Naor, 2000; Guttman et al., 2016). Based on major element ratios (e.g., Na/Cl, SO_4/Cl), Burg and Naor (2000) and Burg and Guttman (2019) have suggested that the groundwater and spring salinization was derived from historic leaking of industrial effluents, of which the Rotem phosphate mine wastewater from MRI was the predominant source. Amiel et al. (2021) used a selection of trace metals defined as Technology-Critical Elements (TCE) detected in the Ein Bokek spring to also suggest contamination from the phosphate mining effluents.

2.2. Sample collection and preparation

To evaluate the utility of Sr isotope geochemistry as a new tracer to detect phosphate mining wastewater, this study investigated: (1) representative phosphate rocks from the producing phosphate ore in Rotem field (n = 4); (2) representative aquifer carbonate rocks from the Zafit formation that compose the upper part of the regional Upper Cretaceous carbonate aquifer in the northeastern Negev (n = 4); (3) wastewater from the MRI phosphate mine that were collected and analyzed for major elements in 2018 (n = 6) and also collected and analyzed for major elements, trace elements, and Sr isotopes in 2021 (n = 7); (4) saline groundwater from Efe'13a and Ein Bokek that previous studies (Burg and Gavrieli, 2013; Burg and Guttman, 2019) have suggested to be contaminated by the Rotem mine wastewater (defined as "impacted water"; n = 3); (5) naturally-occurring saline groundwater (chloride content of

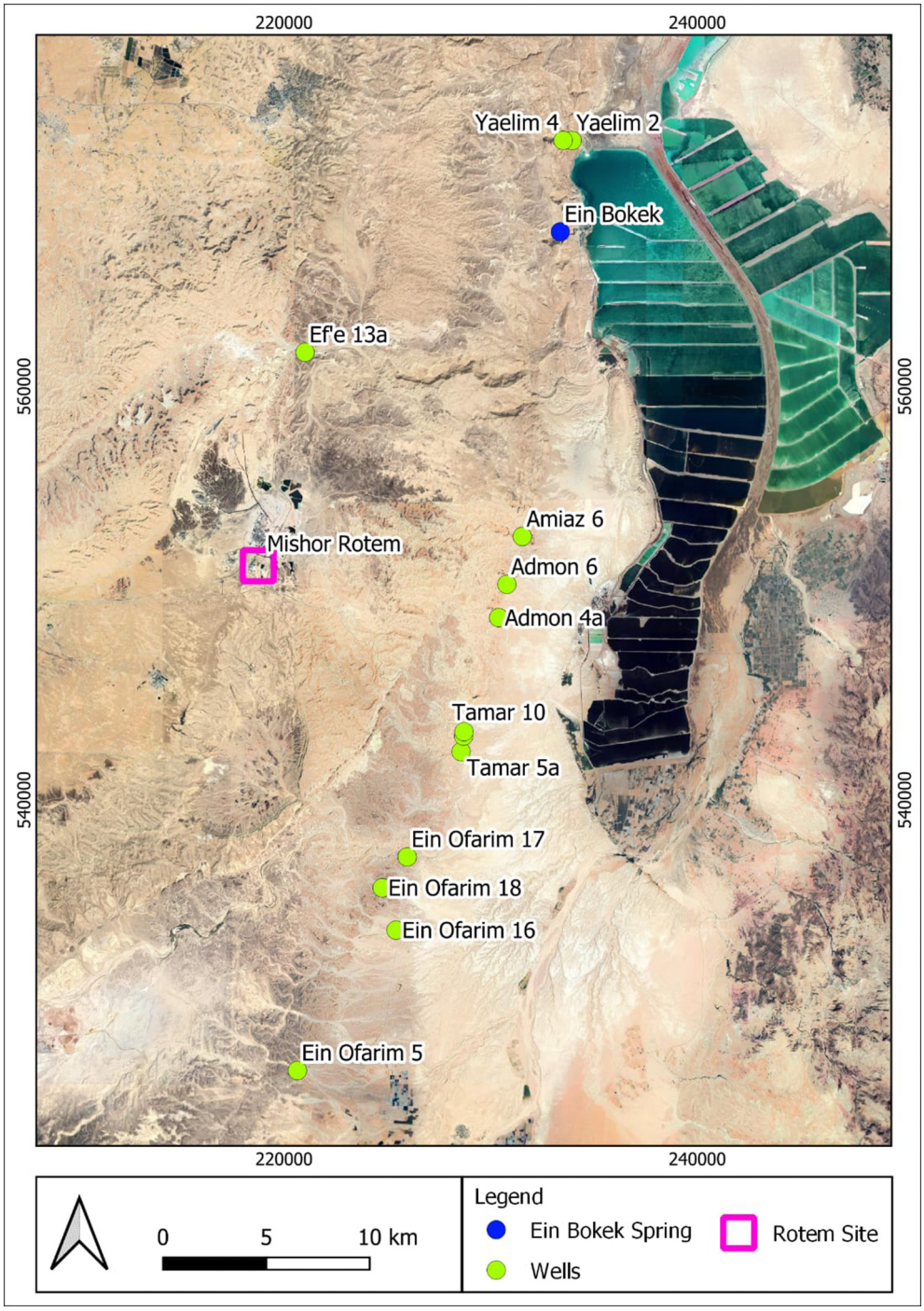

Fig. 1. Location map of Mishor Rotem Industries (MRI) and water sources of Ein Bokek and wells investigated in this study.

645–1900 mg/L; Rosenthal et al., 2007) from the Judea Group aquifer (n = 9); and (6) hypersaline groundwater (chloride content of 5700 to 63,000 mg/L) in the Judea Group aquifer salinized by naturally occurring deep Ca-chloride brines along the Rift Valley (Vengosh et al., 2007; Vengosh and Rosenthal, 1994; n = 7; Fig. 1; Table S1). Water samples were collected following the U.S. Geological Survey sampling protocol (Wilde, 2008); samples analyzed for dissolved anions, cations, trace metals, and Sr isotopes were filtered using 0.45 μm syringe filter units. Cation and trace metal samples were preserved in the field with Optima nitric acid to pH <2 in acid-washed high-density polyethylene (HDPE) bottles. Rock samples were oven-dried at 40 °C until reaching a constant weight and were passed through a 2-mm stainless-steel sieve for homogenization. A subset of each sample was ground using a ceramic mortar and pestle to pass a 200-mesh stainless-steel sieve for subsequent chemical and isotopic analyses.

2.3. Chemical and isotopic analysis

Major elements in the wastewater samples were analyzed by the commercial BACKTOCHEM Lab (Israel). Major elements of the natural water samples were analyzed by ion chromatography (IC) on a Dionex IC DX-2100 system at Duke University. The IC calibration was verified using a secondary Dionex 7-anion and cation standards at varying concentrations. Trace elements in the rock, wastewater and groundwater samples were

Table 1
Strontium isotopes results of phosphate (Mishash Formation) and carbonate rocks (Zafit Formation, Judea Group aquifer) investigated in this study.

Source	Sr (mg/kg)	Sr/Ca	$^{87}Sr/^{86}Sr$
Phosphate rocks			
R1	1078	3.18×10^{-3}	0.707827
R2	1005	3.07×10^{-3}	0.707854
R3	1488	4.40×10^{-3}	0.707764
R4	1472	4.35×10^{-3}	0.707731
Aquifer carbonate rocks			
Crab 1A	87	2.59×10^{-4}	0.707789
Carb 1B	102	2.97×10^{-4}	0.707858
Carb 2A	203	9.2×10^{-4}	
Carb 2B	82	2.29×10^{-4}	0.707822

measured on a Thermo Fisher X-Series II inductively coupled plasma mass spectrometer (ICP-MS) at Duke University. Rock samples were digested in an HF-HNO_3 mixture, and the details of sample digestion and instrumental analysis are described in a previous study (Vengosh et al., 2019). The efficiency of digestion and accuracy of measurement were assessed by measuring the European Commission Phosphate Rock BCR-032 standard. The ICP-MS instrument was calibrated to the National Institute of Standards and Technology 1643f standard, which was used at varying concentrations before, after, and throughout sample runs. Internal standards of In, Tm, and Bi were spiked into all samples and calibration standards prior to measurement on the ICP-MS. Water samples were diluted by different magnitudes to address the large salt matrix variations in the samples collection (i.e., hypersaline wastewater relative to the natural water samples), and the reported data represent the most accurate combination and optimization of water sample dilution that was within the range of the external standards used to verify the results.

Strontium isotope ratios were measured using thermal ionization mass spectrometry (TIMS) on a ThermoFisher Triton at Duke University. Strontium in samples (i.e., bulk water and digested rock solution) was preconcentrated by evaporation in a HEPA-filtered clean hood and re-digested in 3.5 N HNO_3 and then was separated using an Eichrom Sr-specific resin. The $^{87}Sr/^{86}Sr$ ratios were collected in positive mode on the TIMS and the standard NIST SRM 987 had an external reproducibility of 0.710254 ± 0.000012 (2SD, $n = 51$).

3. Results and discussion

3.1. Strontium isotopic characterization of phosphate mining and aquifer rocks

Previous studies have suggested that the Sr isotope ratios of sedimentary phosphorite rocks often mimic the $^{87}Sr/^{86}Sr$ ratios of pore water associated with the early diagenetic stages of phosphate formation, which was assumed to be identical to the composition of the contemporaneous seawater (Compton et al., 1993; Mallinson et al., 1994; McArthur et al., 1990; Stille et al., 1994). The Sr isotope ratios of the phosphate rocks reported in this study (0.707794 ± 5 × 10^{-5}; $n = 4$; Table 1) are consistent with previous Sr isotope data of phosphate rocks from the Mishash Formation in Israel, which reflects the original seawater composition

Table 2
Major elements and Sr isotope data of wastewater from MRI, impacted water of Efe 13a and Ein Bokek, and two types of background saline and hypersaline groundwater from Judea Group aquifer.

Site	Date	pH	TDS	HCO_3	Cl	Br	NO_3	SO_4	Na	K	Mg	Ca	P	Sr	Sr/Ca (x10^{-2})	$^{87}Sr/^{86}Sr$
Phosphate wastewater																
Dekel reservoir	1/8/21	7.6	13,370	244	4154	n.a.	n.a.	n.a.	1234	107	169	2125	<0.5	24.2	1.14	n.a.
Dekel reservoir	23/7/18	7.3	12,979	n.a.	6865	11	n.a.	1600	2280	120	257	1846	n.a.	n.a.	n.a.	n.a.
Acid reservoir D2	1/8/21	<1	548,320	n.a.	146,275	n.a.	n.a.	n.a.	15,765	6508	35,228	49	85,372	2.9	5.99	0.707822
Acid reservoir G2	1/8/21	<1	391,740	n.a.	87,296	n.a.	n.a.	n.a.	678	329	13,065	994	79,923	21.6	2.17	0.707812
Acid reservoir G2	23/7/18	<1	106,214	n.a.	50,410	470	n.a.	38,600	2912	895	11,698	1229	n.a.	n.a.	n.a.	n.a.
Acid reservoir G1	23/7/18	1.0	105,958	n.a.	50,635	485	n.a.	38,900	2934	663	10,536	1805	n.a.	n.a.	n.a.	n.a.
Basic reservoir D3	1/8/21	9.7	252,620	5000	53,363	n.a.	n.a.	n.a.	129	1154	<5	12	688	n.a.	n.a.	n.a.
Basic reservoir D3	23/7/18	9.5	128,421	n.a.	37,725	260	n.a.	8800	80,815	804	3	14	n.a.	n.a.	n.a.	n.a.
Process pipeline to plant	1/8/21	1.5	90,380	n.a.	2432	n.a.	n.a.	n.a.	1508	363	240	6153	24,961	151.4	2.46	0.707776
Drain Pool 5	1/8/21	1.0	69,780	n.a.	3439	n.a.	n.a.	n.a.	1805	505	418	4078	16,813	85.4	2.09	0.707781
Drain Pool 5	23/7/18	<1	13,312	n.a.	905	n.a.	n.a.	7000	1785	187	132	3303	n.a.	n.a.	n.a.	n.a.
Process pipeline from the plant	1/8/21	n.a.	10,159	n.a.	2481	n.a.	n.a.	n.a.	1493	340	240	5605	26,244	155.0	2.77	0.707755
Process pipeline from the plant	23/7/18	<1	13,129	n.a.	848	2	n.a.	6600	1649	223	175	3634	n.a.	n.a.	n.a.	n.a.
Impacted water																
Efe 13a well water	13/1/21	5.9	n.a.	n.a.	8405	146	11	629	1203	88	947	2523	0.1	24.0	0.95	0.707951
Ein Bokek	29/7/21	7.7	8442	146	4998	86	7	408	595	35	569	1605	<0.1	17.4	1.08	0.707951
Ein Bokek	28/6/18	7.5	8380	169	4753	84	n.a.	496	671	31	554	1622	n.a.	15.8	0.97	0.707945
Background saline groundwater																
Ein Ofarim 5	29/7/21	7.0	1852	110	645	3	1.6	446	362	22	75	190	<0.1	3.7	1.94	0.707771
Ein Ofraim 17	29/7/21	7.0	3436	305	1357	9	3.5	636	671	32	141	285	<0.1	6.4	2.26	0.707815
Ein Ofraim 18	29/7/21	7.2	3461	317	1376	7	1.2	621	677	32	153	277	<0.1	6.5	2.35	0.707818
Ein Ofraim 18	28/6/18	6.9	3254	326	1225	4	n.a.	592	655	29	150	274	n.a.	5.9	2.15	0.707812
Ein Ofraim 16	28/6/18	7.0	3119	314	1131	4	n.a.	628	589	25	138	290	n.a.	6.2	2.15	0.707786
Tamar 5a	29/7/21	6.9	3747	281	1488	10	4.2	733	747	36	158	292	<0.1	6.5	2.21	0.707836
Tamar 12	29/7/21	7.0	4604	305	1927	14	4.0	768	992	44	208	347	<0.1	7.5	2.16	0.707831
Tamar 10	29/7/21	6.6	4632	281	1897	14	2.7	820	994	51	218	358	<0.1	7.1	1.98	0.707839
Adamon 4a	29/7/21	6.9	3695	293	1354	7	3.1	675	1001	50	94	221	0.7	6.0	2.71	0.707789
Zohar 16	29/7/21	7.1	3220	268	1195	8	3.8	659	694	59	126	211	0.2	9.1	4.29	0.707756
Background hypersaline groundwater																
Amiaz 6	28/7/21	6.4	11,600	284	5772	82	n.a.	1274	2672	165	535	816	n.a.	14.4	1.76	0.707933
Admon 6	29/7/21	6.6	15,559	244	8871	139	16.7	1049	3200	205	747	1144	1.2	24.3	2.12	0.707938
Zohar 4a	29/7/21	7.0	24,088	256	14,795	297	28.3	818	4185	366	1998	1372	<0.1	31.8	2.32	0.707970
Yeelim 2	29/7/21	6.1	89,286	159	60,763	1617	90	787	9598	1683	10,315	4362	0.9	97.1	2.32	0.707987
Yeelim 4	29/7/21	5.9	93,747	171	63,181	1624	87	548	10,452	1713	11,346	4712	<0.1	101.1	2.15	0.708007
Yeelim 4	28/6/18	5.9	80,994	167	51,885	1250	n.a.	653	10,823	1613	10,244	4358	n.a.	80.6	1.85	0.707963

n.a. denotes not available.

of the paleoenvironment of the phosphate deposition during the Campanian (Late Cretaceous) (Soudry et al., 2006). The Sr isotope ratios of the acidic and saline phosphate wastewater from MRI (mean = 0.707789 ± 3×10^{-5}; $n = 5$; Table 2) are almost identical to the isotope ratios of the phosphate rocks (Fig. 2). This confirms that dissolution of the phosphate rocks does not induce any selective mobilization of Sr, and therefore, the original Sr isotope composition of the phosphate rocks is maintained in the phosphate wastewater. It is important to emphasize that while different chemical processes and methodologies of phosphate extraction may generate different wastewater chemistry, it is not expected to affect the distinctive Sr isotope ratios of the phosphate ore specifically due to the relatively high concentrations of Sr on the phosphate rocks (1000–1500 mg/kg; Table 1).

Release of the phosphate wastewater into the environment is expected to influence the Sr isotope ratio of most natural waters, owing to its high Sr concentration. For example, in the case study of the saline groundwater in Judea Group aquifer, the Sr concentration in the phosphate wastewater (an average of 73.4 mg/L; Table 2) is 12-fold higher relative to that in the saline groundwater (6.2 mg/L). Therefore, contamination from the phosphate mine wastewater would modify the original Sr isotope composition of the impacted water towards the composition of the phosphate rocks, in a scenario where the initial isotopic composition of the impacted water is different from that of the wastewater.

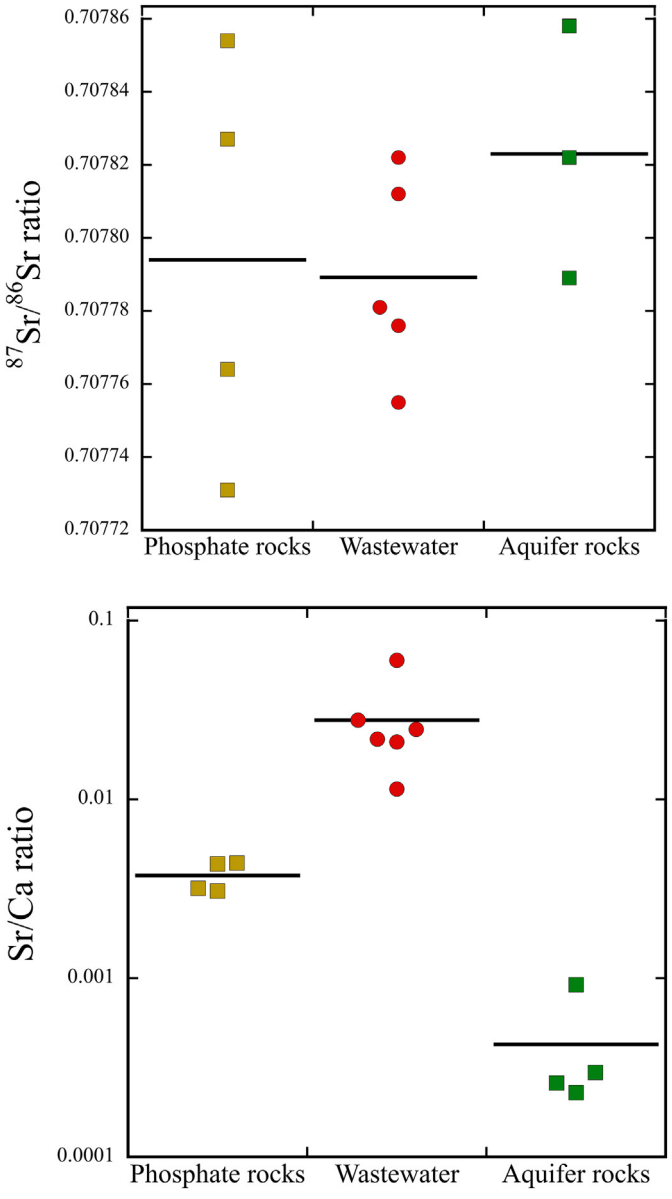

Fig. 2. Distribution of strontium isotope ratios and Sr/Ca ratios in the Rotem phosphate rocks, phosphate acidic wastewater, and the carbonate rocks of Judea Group aquifer (Zafit Formation). The black lines indicate median values.

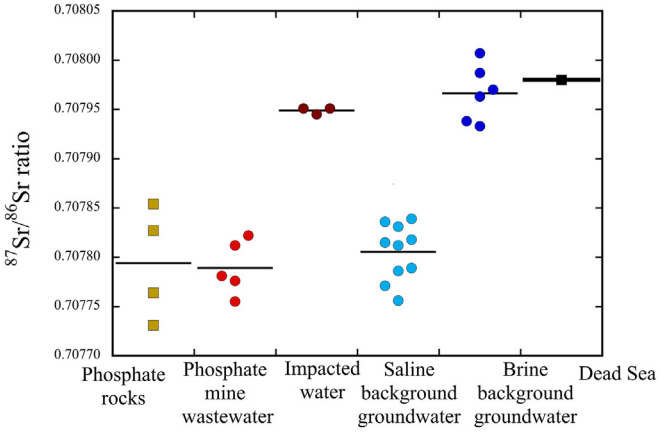

Fig. 3. Distribution of strontium isotope ratios in the Rotem phosphate rocks and the different water sources in this study, including phosphate wastewater, impacted water (Ein Bokek and Efe 13a), saline background water, and hypersaline (brine) background water in comparison to the composition of the Dead Sea. The Dead Sea data is from Stein et al. (1997). The black lines indicate median values.

It is important to emphasize that the retention of Sr through adsorption to clay minerals and oxides and/or secondary precipitation in the aquifer would not modify the Sr isotope ratios in the groundwater. This contrasts with the dissolved P and trace elements whose concentrations can be greatly affected by water rock interactions. The only possible modification of the Sr isotope composition in groundwater is dissolution of the aquifer rock that could potentially modify the original isotopic ratios of the phosphate effluents in the contaminated water. For the case study of the Judea Group aquifer, the range of $^{87}Sr/^{86}Sr$ ratios of the aquifer rocks (Zafit Formation) overlap with that of the phosphate rocks (Fig. 2; Table 1). Therefore, dissolution of the aquifer rocks would have resulted in similar $^{87}Sr/^{86}Sr$ ratios as the Sr isotope fingerprint of the phosphate wastewater. Previous studies have recognized that the potential modification of the original $^{87}Sr/^{86}Sr$ ratio due to dissolution of aquifer rocks is an inherent limitation of the Sr isotope tracer (Vengosh et al., 2016). Nonetheless, given the high salinity, high Sr concentrations, and an order of magnitude higher Sr/Ca ratios of the phosphate wastewater relative to the carbonate aquifer rocks (Fig. 2), we expect only a minimum impact of this type of water-rock interactions on the Sr isotope composition of the contaminated water.

Table 3
Data on the sources and salinity of the industrial wastewater historically disposed in Ramat Rotem. Based on data reported in Burg and Naor (2000).

Source	Wastewater volume (million cubic meter)	Chloride (mg/L)	Origin of the industrial wastes
Gypsum pool	4.5	630	Rotem phosphate mine
Periclas Lake	1.5	60,000	Periclas Industry
Lake A	1.24	83,000	Rotem phosphate mine
Lake B	1.31	60,000	Rotem phosphate mine
Sinkhole	0.1–0.2	30,000	Periclas Industry
Total	8.75		

3.2. Tracing the phosphate mining effluents in northeastern Negev

In the northeastern Negev, historic discharges, and apparent leaking of Rotem wastewater from MRI have been implicated in the contamination of downstream groundwater as reflected in salinization of shallow groundwater in Efe 13a and the discharge spring of Ein Bokek (Fig. 1; Burg and Gavrieli, 2013; Burg and Guttman, 2019; Burg and Naor, 2000; Guttman et al., 2016). The results of this study show that the $^{87}Sr/^{86}Sr$ ratios of the impacted water of Efe 13a and Ein Bokek ($0.707949 \pm 3 \times 10^{-6}$; Table 2) are much higher than the Sr isotope ratios of the phosphate rocks and wastewater (Fig. 3). Instead, the $^{87}Sr/^{86}Sr$ ratios of Ein Bokek and Efe 13a are within the $^{87}Sr/^{86}Sr$ range of the background highly saline Ca-chloride groundwater (0.70793 to 0.70801; Table 2) and the naturally occurring brines from the Dead Sea (0.70803; Stein et al., 1997), which would suggest salinization from a "Dead Sea-like" brine source. The $^{87}Sr/^{86}Sr$ ratios measured in samples from Ein Bokek collected in 2018 and 2021 were identical (Table 2), reflecting the consistent Sr source to this spring between the sampling years. Therefore, the Sr isotope data are not consistent with previous assumptions that the salinization of Efe 13a and Ein Bokek primarily originated from the historic leaking of phosphate wastewater from MRI.

One of the major assumptions made by Burg and Guttman (2019) was that the highly acidic wastewater interacted with the aquifer rocks and caused modification of the original Ca/Mg ratios and retention of metals that are enriched in the acidic wastewater (see below). This was the major explanation for the inconsistency between relatively high salinity and low concentrations of metal(loid)s in Ein Bokek compared to the high trace element concentrations in phosphate wastewater. However, such water-rock interactions would produce a groundwater Sr isotope ratio closer to the aquifer rock composition, similar to the Sr isotope composition of the background saline groundwater (Fig. 3). In contrast, the $^{87}Sr/^{86}Sr$ ratio of the impacted water is much higher than that of the aquifer rocks and background saline groundwater, ruling out the possibility of modification towards the aquifer rocks composition with lower $^{87}Sr/^{86}Sr$ ratios. Instead, the close similarity of the $^{87}Sr/^{86}Sr$ ratios in the impacted water to the $^{87}Sr/^{86}Sr$ ratios of the Dead Sea brines suggests salinization from a different saline source with the Dead Sea Sr isotope composition.

Previous studies have estimated that the annual wastewater volume that was historically discharged to the reservoirs at MRI was 7.5 million cubic meter (MCM) per year, from which 2.5 MCM per year infiltrated and leaked into the subsurface. Since this operation lasted for about 30 years, it was estimated that a volume of about 75 MCM of industrial wastewater infiltrated into the subsurface and had caused the downstream contamination of Efe 13a and Ein Bokek (Burg and Naor, 2000; Burg and Guttman, 2019). According to these studies, the wastewater effluents originated from two major sources: the Rotem phosphate mining and the magnesium oxide (Periclas) industry with effluents composed of modified Dead Sea brines, defined as Dead Sea Water Type (DSWT). The two types of wastewaters were clearly distinguished by their chemical composition; the Periclas wastewater resembled the composition of the Dead Sea brine with high Br/Cl and low SO_4/Cl ratios, whereas the Rotem wastewater had lower Br/Cl and high SO_4/Cl ratios (Arad and Helitz, 1992; Burg and Naor, 2000). We observed similar results of lower Br/Cl and higher SO_4/Cl in the Rotem wastewater collected in this study (see below), indicating consistency of the geochemical composition over time. Based on the 1990 data reported by Arad and Halicz (1994), Burg and Naor (2000) reconstructed the volume and chemical compositions of the two types of the industrial wastewaters (Table 3). Based on the chemical data (e.g., Br/Cl, SO_4/Cl, phosphorous concentrations) reported in Burg and Naor (2000), one can distinguish between the Rotem effluents that annually contributed 7.05 MCM relative to Periclas wastewater that contributed 1.7 MCM (Table 3). Therefore, based on historical data, the Rotem wastewater accounted for about 80 %, while Periclas only made up 20 % of the total industrial wastewater that was historically discharged from MRI.

The major assumption made in previous studies was that a fraction of the industrial effluents that were discharged to the reservoirs in MRI,

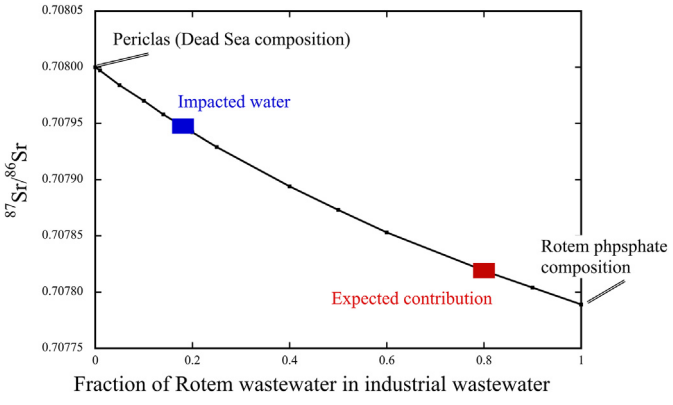

Fig. 4. Theoretical mixing model between Rotem and Periclas wastewaters sources. We conducted mass-balance calculations assuming that the Periclas wastewater had the strontium isotope ratio identical to that of the Dead Sea brine. Based on the relative contribution of the Rotem wastewater (80 % of the total volume of wastewater, see Table S3) the $^{87}Sr/^{86}Sr$ ratio of the mixed solution would have been much lower (red square) than the $^{87}Sr/^{86}Sr$ ratios measured in Ein Bokek and Efe 13a (impacted water; blue square), indicating a much lower contribution, if any, of the phosphate wastewater.

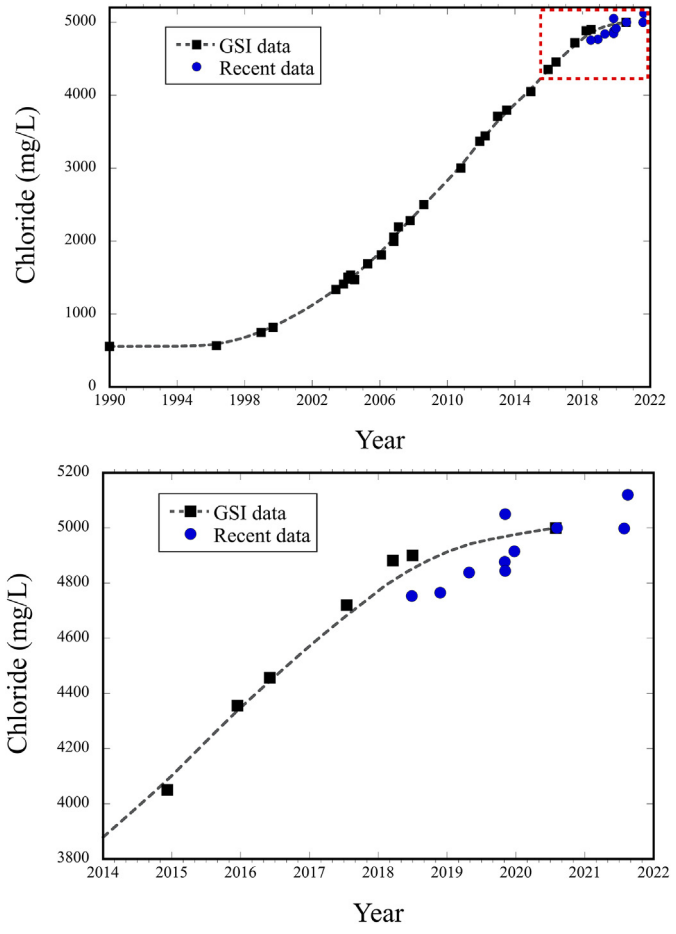

Fig. 5. Changes in salinization rates of Ein Bokek spring over time as measured by the Israel Geological Survey (GSI) and recent (2018–2021) sampling. Between late-1990s and 2018 the salinization rate was 240 mgCl/L per year, while since 2018 the salinization rate decreased to 51 mgCl/L per year. The red dashed square in the upper panel is shown in the lower panel.

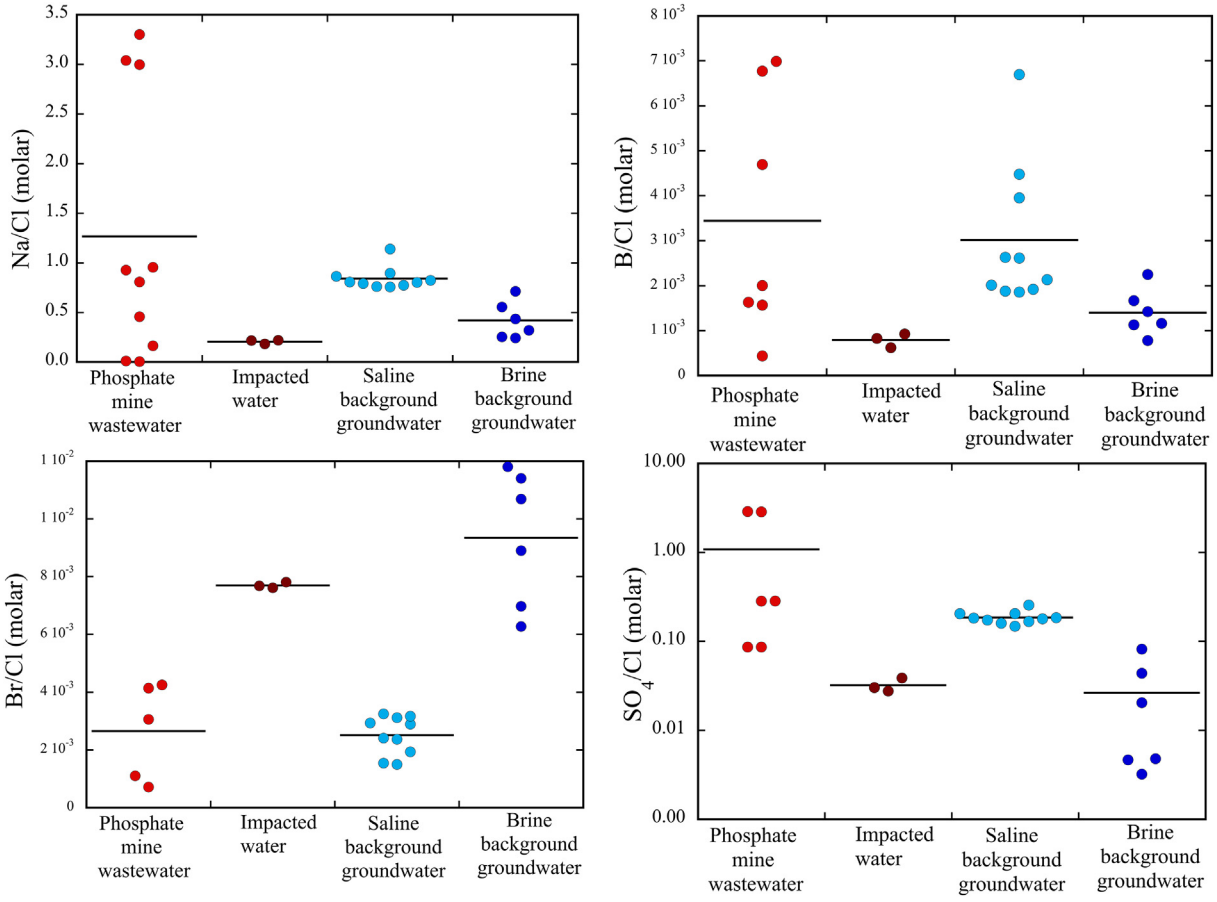

Fig. 6. Variations of geochemical parameters of Na/Cl, Br/Cl, SO_4/Cl and B/Cl (molar) ratios of the different water resources investigated in this study. The black lines indicate median values.

leaked and infiltrated into the subsurface, with an estimate recharge of 2.5 MCM per year. This was the basis of the geochemical model postulated by Burg and Guttman (2019) that included blending of both Rotem and Periclas wastewaters to generate a hypothetical mixture solution with Na/Cl and SO_4/Cl ratios to reflect the mixing proportions of the two wastewater sources. We test this model by using the strontium isotopes mass-balance between the phosphate wastewater and the Periclas wastewater, assuming that (1) the mean values of Sr concentrations (75 mg/L) and $^{87}Sr/^{86}Sr$ (0.70779) in the recent phosphate wastewater represent also the historical composition of the Rotem wastewater; (2) the Sr/Ca ratio (1.88×10^{-2}) and the $^{87}Sr/^{86}Sr$ (0.7080) of the modern Dead Sea (Stein et al., 1997) represent the historical composition of the Periclas wastewater; and (3) the Ca content of Periclas wastewater that was discharged to a leaking sinkhole (2500 mg/L) reported by Burg and Naor (2000) can be used to estimate the Sr content in the Periclas wastewater, which based on the Dead Sea Sr/Ca ratio would be equal to 48 mg/L. Based on this mass-balance calculation, leaking of all the industrial wastewaters at the same proportion as described in the previous studies (i.e., 80 % Rotem versus 20 % Periclas wastewaters; Table 3) would generate a blend with a $^{87}Sr/^{86}Sr$ ratio of 0.70782 (Fig. 4). This ratio is different than the $^{87}Sr/^{86}Sr$ ratio measured in Ein Bokek and Efe 13a ($0.707949 \pm 3 \times 10^{-6}$; Fig. 4). Instead, the mass-balance calculations indicate that the ratio measured in Ein Bokek and Efe 13a would reflect a much lower (<20 %) contribution from the Rotem phosphate mining wastewater. Consequently, the basic assumption of previous studies that the blending of the two types of industrial wastewaters had caused the contamination of Efe 13a and Ein Bokek is not consistent with the Sr isotope data, which suggest a predominance of infiltration of Periclas wastewater with the Dead Sea Sr isotope fingerprint. Since the volume of the Periclas wastewater that was discharged to the reservoirs and released at the sink hole was much smaller and consisted of only 20 % of the total wastewater volume (Table S3), the estimates of an annual leaking volume of 2.5 MCM per year seems to be an overestimate of the actual volume of the leaking Periclas wastewater that infiltrated into the aquifer and had caused the salinization of Efe 13a and Ein Bokek. In summary, the Sr isotope data suggest a different source and a much smaller volume of industrial wastewater infiltration than previously suggested.

Integrating recent (2018–2021) measurements with available historical chloride concentration data conducted by the Israel Geological Survey

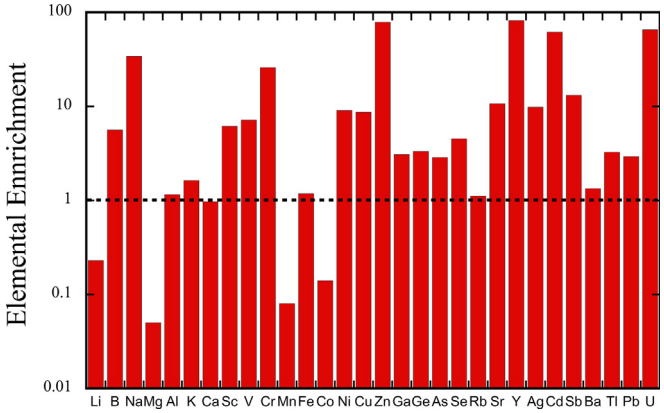

Fig. 7. Enrichment of elements in the Rotem phosphate rocks in comparison to their concentrations in the Judea Group aquifer carbonate rocks (Zafit Formation).

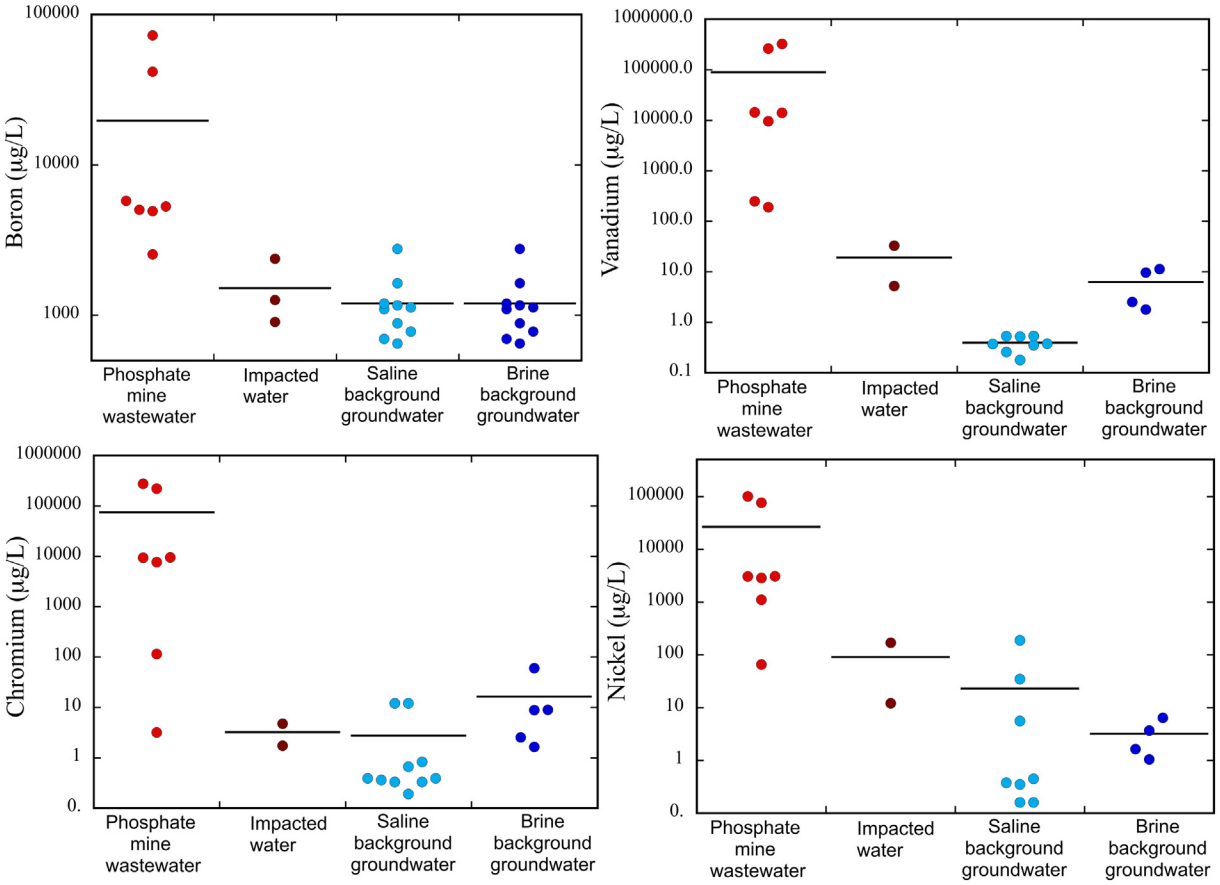

Fig. 8. Trace elements concentrations (logarithmic scale) in Rotem phosphate wastewater, impacted water (Ein Bokek and Efe 13a), background saline groundwater, and background hypersaline (brine) groundwater from the Judea Group aquifer. The black lines indicate median values.

(GSI) shows that the salinization rate of Ein Bokek has decreased since 2018 (Fig. 5). Between 2003 and 2018 the average salinization rate was 240 mg Cl/L per year, while since 2018, it was only 51 mg Cl/L per year, representing a nearly 5-fold decline (Fig. 5). This evident reduction of salinization rates at Ein Bokek suggests that the balance between the saline water and regional low-saline groundwater in the aquifer has shifted towards a lower proportion of the saline source, and natural remediation of the salinity in the aquifer may have started. This finding is consistent with the indication that the volume of the saline effluents that historically infiltrated into the subsurface was apparently smaller than previously estimated.

3.3. Geochemical characterization of phosphate mining effluents

The phosphate mine wastewater is characterized by high acidity (pH < 1), high salinity (TDS up to 548,000 mg/L), and very high metal(loid) concentrations, many in the mg/L (ppm) level (Table 2 and Table S1; Figs. 6 and 7). The phosphate wastewater from MRI is also characterized by a wide range of Na/Cl ratios (0.01 to 3.3; reported as molar ratios), relatively high SO_4/Cl ratios (0.1–0.5), relatively low Br/Cl ratios (7.1×10^{-4} to 4.3×10^{-3}) and high B/Cl ratios (4×10^{-4} to 7×10^{-3}) compared to these ratios in the impacted water (Na/Cl = 0.13, Br/Cl = 8.9×10^{-3}, SO_4/Cl = 9×10^{-3}; B/Cl = 7.9×10^{-4}) (Fig. 6). Similar high salinity and sulfate levels were recorded in wastewater collected in early 1990s in MRI (Arad and Halicz, 1994). Given the conservative characteristics of both Cl and Br, one would assume that the original Br/Cl ratio of the saline source would be preserved in the salinized water and not be affected by water-rock interactions. Likewise, the relatively high SO_4/Cl ratio that characterizes the phosphate wastewater is expected to be persevered in the shallow oxidized groundwater and Ein Bokek spring, particularly given that the elevated U concentrations in the shallow groundwater indicate oxic conditions (see discussion below). Yet both Efe 13a and Ein Bokek spring show higher Br/Cl and lower SO_4/Cl ratios compared to the Rotem wastewater (Fig. 6), which suggests a different salinity source.

To evaluate the enrichment of metal(loid)s in the phosphate rock, we compared their concentrations in the Rotem phosphate rocks to those of the local aquifer carbonate rocks of Zafit Formation from Judea Group aquifer (Table S2). The data show enrichment of several metal(loid)s in the phosphate rocks relative to the carbonate aquifer rocks, in particular B (by a factor of 6), Cr (26), Ni (9), Cu (9), Zn (79), Sr (11), Y (82), Cd (62), Sb (13), and U (65) (Fig. 7). This is consistent with previous studies that have reported elevated levels of these elements in phosphate rocks (Batarseh and El-Hasan, 2009; Jiries et al., 2004; Kratz et al., 2016; Schnug and Haneklaus, 2015; Silva et al., 2010; Sun et al., 2020). Consistently, high concentrations of these metal(loid)s were also detected in the phosphate wastewater, with trace element concentrations at the ppm level, several orders of magnitude higher than those in the background saline and highly saline groundwater (Table S1, Fig. 8).

3.4. The occurrence of metal(loid)s in salinized groundwater

A systematic analysis of the metal(loid) occurrences in Rotem phosphate wastewater, impacted waters, the background saline groundwater, and the hyper saline (brine) groundwater show that elements enriched in phosphate rocks including B, Cr, Ni, Cu, Zn, Sr, Y, Cd, Sb, and U (Fig. 7) also had elevated concentrations in the phosphate wastewater from MRI,

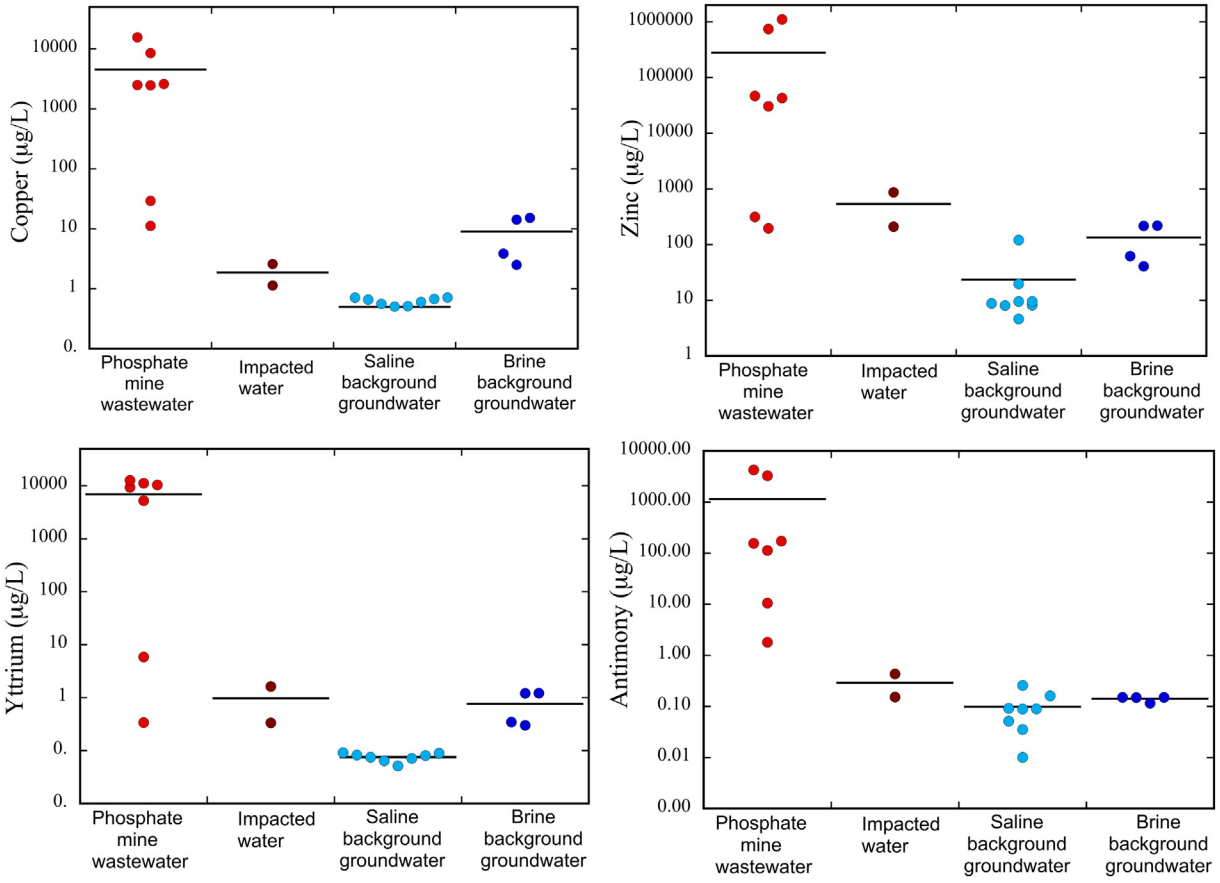

Fig. 8 (*continued*).

in most cases at the ppm levels (Fig. 8; Table S1). In contrast, their concentrations in the impacted waters were several orders of magnitude lower (Fig. 8; Table S1). In addition, the concentrations of these elements in the two types of the naturally occurring background groundwater were mostly similar to, or even higher than those in the impacted water (Fig. 8). Only Cd and U showed relatively higher concentrations in the impacted water as compared to the background groundwater, although U and Cd concentrations in the background groundwater were not negligible or non-detectable. Similarly, trace elements that were not particularly enriched in the phosphate rocks but show high concentrations in the phosphate wastewater (such as Mo, V, and As), show consistent similar and even higher contents in the background groundwater relative to their concentrations in the impacted waters (Fig. 8; Table S1). Therefore, the trace elements data alone cannot definitively establish the connection between the impacted water and the phosphate wastewater. Similarly, the phosphate wastewater contains high concentration of dissolved phosphorus (up to 80,000 mg/L), whereas the impacted water showed no traces of P, while several background groundwater samples had non-detectable concentrations (Table 2). This observation indicates that using the concentrations of P alone cannot be used as an indicator for possible contamination by phosphate wastewater, further reinforcing the importance of using an independent geochemical tracer such as Sr isotopes.

Previous studies have suggested that the low levels of metal(loid)s in Ein Bokek resulted from interactions between acidic effluents and the aquifer rocks that had caused the trace elements retention through secondary precipitation, which would explain their elimination in the contaminated groundwater (Arad and Halicz, 1994). Therefore, the use of trace elements to detect the possible impact of phosphate wastewater on the environment is questionable given the possible water-rock interactions and the variable geochemical characteristics of different elements (e.g., cationic elements versus oxyanions) that would change their solubility, and consequently, their occurrence in the impacted water. It is also important to note that the occurrence of some metal(loid)s in groundwater such as hexavalent uranium depends on the redox state of the water, since uranium is not soluble under reducing conditions. Therefore, uranium concentrations in groundwater are not only dependent on the concentration in the apparent contamination source, but also on the ambient geochemical conditions in the aquifer (Vengosh et al., 2022). The higher concentrations of uranium in Ein Bokek and Efe 13a relative to the background groundwater can be explained by the difference between the shallow and more oxidized groundwater that characterize Efe 13a and Ein Bokek relative to the deep and more reduced background groundwater from deeper wells. This can also explain why other metalloids that are more soluble under reducing conditions such as As and Mo were more abundant in the background groundwater collected from deeper wells relative to the shallow impacted groundwater of Efe 13a and Ein Bokek (Fig. 8; Table S1). These geochemical properties are essential in evaluating the occurrence of metals and metalloids in groundwater resources, and one cannot simply assume that high concentrations of some metals in a groundwater resource are derived primarily from a presumably contamination source without considering the ambient redox conditions of the aquifer.

We further analyzed the trace elements defined by Amiel et al. (2021) as Technology-Critical Elements to determine if their abundance in the impacted water can be used to detect the source of contamination and the link to the phosphate mining wastewater. A detailed analysis of the variations of these elements (Table 4) shows that some elements were not detectable (Ga), or their concentrations in the impacted waters were very low or close to the detection limit (Rh). Furthermore, the concentrations of some

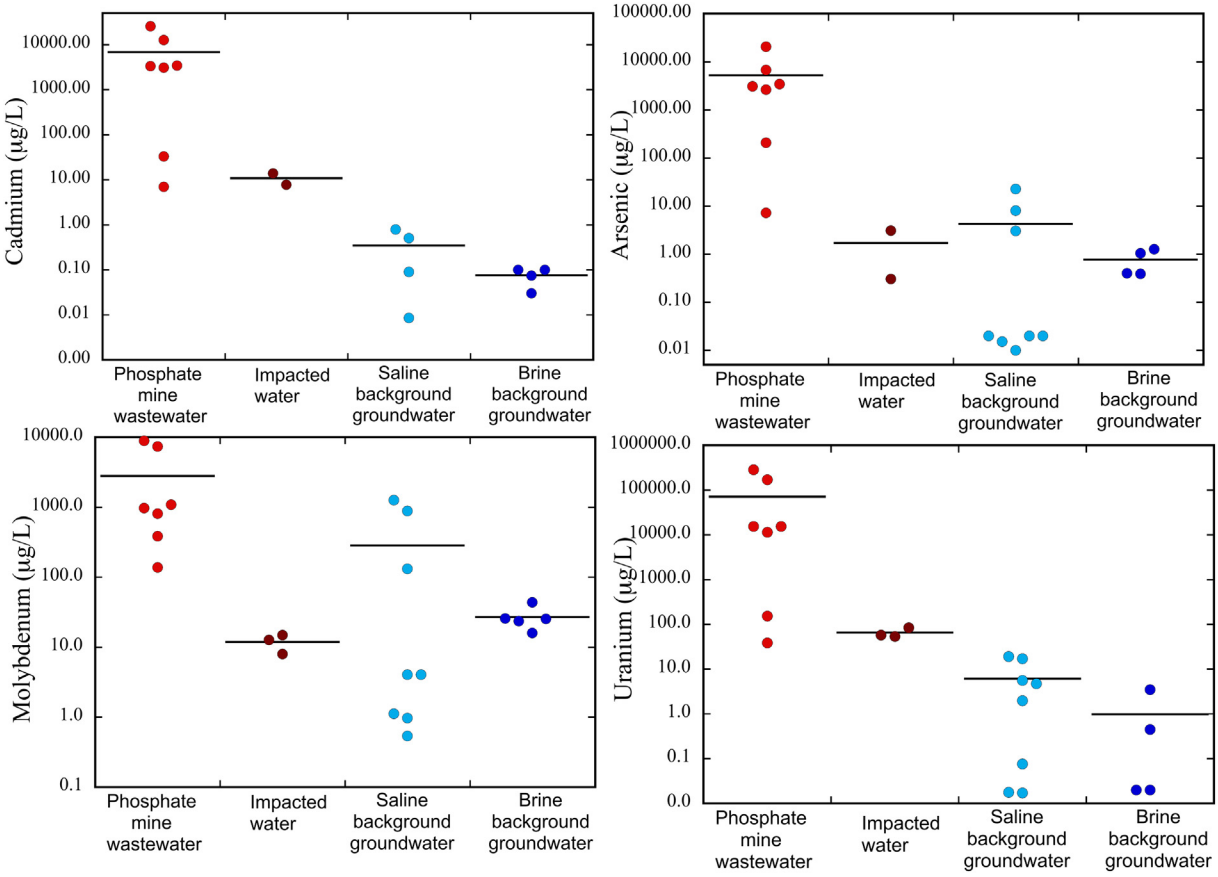

Fig. 8 (*continued*).

of these elements (Rh, Tl) in the phosphate rocks and the associated wastewater were also very low (Table 4), and thus the phosphate wastewater is not a likely source for these elements in the impacted water. Importantly, the concentrations of some of the Technology-Critical Elements in the background groundwater, including Ge, Y, Rh, and Tl were similar, or even higher than that of the impacted water (Table 4). Therefore, given the ubiquitous occurrence of these elements in the regional and non-contaminated groundwater, the occurrence of these elements in the impacted water is not unique and cannot be linked explicitly to the Rotem phosphate wastewater. Overall, the data presented in this study suggest that none of the Technology-Critical Elements proposed by Amiel et al. (2021) can be used as reliable or unique tracers for detecting the impact of phosphate wastewater on the environment.

4. Conclusions

This study presents Sr isotopes as a new geochemical tracer for detecting the impact of phosphate mine wastewater on the environment and the quality of nearby water resources. While previous studies and new data presented in this study show that highly saline and acidic phosphate wastewater associated with phosphate mining and fertilizers production contains elevated levels of P and metal(loid)s that can contaminate associated water resources, multiple geochemical processes could potentially modify the abundances of these metal(loid)s in the impacted groundwater, and thus could mask the ability to identify the migration and the impact of the phosphate wastewater. We show in this study that the Sr isotope ratios of the phosphate wastewater are identical to those of the phosphate rocks and thus can be used as a universal tracer to delineate possible impacts of any phosphate mining on associated water resources. Given the enrichment of Sr in the phosphate wastewater and the 'conservative' geochemical behavior of Sr isotopes that are not modified by secondary water-rock interactions (e.g., adsorption), nor are sensitive to changes in redox state of the water, we suggest that the Sr isotopes can be used as a sensitive and robust tracer for detecting water contamination from phosphate mining. This study utilizes a regional case study in the northeast Negev in Israel, where salinization of groundwater and a spring have been attributed to upstream historic leaking and contamination from phosphate wastewater. The conceptual model for the salinization of Ein Bokek and Efe 13a has been based on major elements data of the salinized groundwater and the assumption that all of the industrial wastewaters were historically leaked from the

Table 4
A detailed comparison of the concentrations of selective Technology-Critical Elements (TCE) previously used with Amiel et al. (2021) in the Rotem phosphate rocks and water sources, including Rotem wastewater, impacted water (Ein Bokek and Efe 13a), background saline groundwater, and background brine-impacted groundwater.

Element	Phosphate rocks (mg/kg)	Rotem wastewater (mg/L)	Impacted water (mg/L)	Background saline groundwater (mg/L)	Background brine groundwater (mg/L)
Gallium (Ga)	0.1–2.9	14–1950	BDL	0.03–0.26 (detectable in 7 out of 9)	BDL
Germanium (Ge)	0.6–0.9	2–1111	0.27–0.33	0.03–0.71 (detectable in 7 out of 9)	0.40–1.04 (detectable in 4 out of 5)
Yttrium (Y)	50–80	6–12,674	0.33–1.62	0.05–0.09 (detectable in 7 out of 9)	0.09–1.21 (detectable in 4 out of 5)
Rhodium (Rh)	BDL	0.14–0.48	0.03–0.05	0.009–0.021 (detectable in 7 out of 9)	0.015–0.405 (detectable in 4 out of 5)
Thallium (Tl)	0.04–0.2	24.7–51.2	6.1–7.0	0.009–3.22 (detectable in 2 out of 9)	5.2 (detectable in 1 out of 5)

reservoirs in MRI to the subsurface to cause the downstream groundwater contamination. Previous findings of low levels of trace elements defined as Technology-Critical Elements (TCE) in the Ein Bokek spring have also been attributed to contamination from Rotem phosphate wastewater. To test the validity of the new proposed Sr isotope tracer, this study presents comprehensive data of major elements, a wide range of 40 trace elements, and Sr isotope ratios that were measured in Rotem phosphate rocks, Judea Group aquifer rocks, and all possible water sources, including Rotem wastewater from MRI, the impacted water of Efe 13a and Ein Bokek, and two types of background groundwater in the Judea Group aquifer. The results of this study indicate that trace elements, including TCEs, ubiquitously occur in the regional and non-contaminated groundwater at the same levels as detected in the impacted waters of Ein Bokek and Efe 13a, and thus the occurrence of these elements in Ein Bokek is not unique and cannot be explicitly linked to the Rotem wastewater. Likewise, despite of high concentrations of P in the phosphate wastewater, P was not detected in the impacted water. In contrast, the Sr isotope data of the impacted water is not consistent with the isotopic fingerprint of the phosphate rocks and associated wastewater, but rather is similar to the composition of the Dead Sea brine. Therefore, the Sr isotope data rule out the previous assumptions that the salinization of Efe 13a and Ein Bokek originated from historic leaking of wastewater primarily derived from the phosphate wastewater. Instead, the new data suggest salinization from another saline source that originated from the DSWT wastewater in MRI. Given the smaller volumes of the historical contribution of DSWT wastewater relative to the overall wastewater, the new finding implies a much smaller volume of the overall industrial waste that was leaked to the subsurface. The evidence for a different source with lower volume is consistent with the observation that the salinization rate of Ein Bokek spring has decreased since 2018, implying dilution of an apparent smaller volume of infiltrated wastewater in the aquifer and beginning of recovery of the salinized aquifer. Overall, this study presents a new geochemical tool that can be used to delineate the impact of phosphate mining and fertilizers formation in the environment.

Supplementary data to this article can be found online at https://doi.org/10.1016/j.scitotenv.2022.157971.

CRediT authorship contribution statement

Avner Vengosh: Conceptualization, Methodology, Validation, Resources, Writing - Original Draft, Writing - Review & Editing, Visualization, Supervision, Funding acquisition. **Zhen Wang:** Methodology, Validation, Investigation, Writing - Review & Editing, Visualization. **Gordon Williams:** Methodology, Validation, Investigation, Writing - Review & Editing, Visualization. **Robert Hill:** Methodology, Validation, Investigation, Writing - Review & Editing, Visualization. **Rachel M. Coyte:** Methodology, Validation, Investigation, Writing - Review & Editing, Visualization. **Gary S. Dwyer:** Methodology, Validation, Investigation, Writing - Review & Editing, Visualization.

Data availability

All data are included in the manuscript and supplement

Declaration of competing interest

The authors declare the following financial interests/personal relationships which may be considered as potential competing interests: Avner Vengosh reports financial support was provided by Rotem Amfert Negev Ltd. Avner Vengosh reports a relationship with Rotem Amfert Negev Ltd. that includes: consulting or advisory.

Acknowledgement

We acknowledge that Rotem Amfert Negev Ltd. paid Duke University for the analytical measurements conducted in this study and that Avner Vengosh was temporarily hired as a consultant by Rotem Amfert Negev Ltd. to evaluate the water quality data of this study. We the reviewers and Editor for a thorough and prompt review.

References

Al-Hwaiti, M.S., Brumsack, H.J., Schnetger, B., 2018. Heavy metal contamination and health risk assessment in waste mine water dewatering using phosphate beneficiation processes in Jordan. Environ. Earth Sci. 77, 661. https://doi.org/10.1007/s12665-018-7845-0.

Amiel, N., Dror, I., Zurieli, A., Livshitz, Y., Reshef, G., Berkowitz, B., 2021. Selected technology-critical elements as indicators of anthropogenic groundwater contamination. Environ. Pollut. 284, 117156. https://doi.org/10.1016/j.envpol.2021.117156.

Arad, A., Halicz, L., 1994. Industrial wastes in the Rotem basin, northern Negev. Israel Geological Survey Current Research. 9, pp. 7–10.

Aydin, I., Aydin, F., Saydut, A., Bakirdere, E.G., Hamamci, C., 2010. Hazardous metal geochemistry of sedimentary phosphate rock used for fertilizer (Mazıdag, SE Anatolia, Turkey). Microchem. J. 96, 247–251. https://doi.org/10.1016/j.microc.2010.03.006.

Batarseh, M., El-Hasan, T., 2009. Toxic element levels in the phosphate deposits of Central Jordan. Soil Sediment Contam. Int. J. 18, 205–215. https://doi.org/10.1080/15320380802660214.

Belgada, A., Charik, F.Z., Achiou, B., Ntambwe Kambuyi, T., Alami Younssi, S., Beniazza, R., Dani, A., Benhida, R., Ouammou, M., 2021. Optimization of phosphate/kaolinite microfiltration membrane using Box-Behnken design for treatment of industrial wastewater. J. Environ. Chem. Eng. 9, 104972. https://doi.org/10.1016/j.jece.2020.104972.

Bigalke, M., Ulrich, A., Rehmus, A., Keller, A., 2017. Accumulation of cadmium and uranium in arable soils in Switzerland. Environ. Pollut. 221, 85–93. https://doi.org/10.1016/j.envpol.2016.11.035.

Bituh, T., Marovic, G., Franic, Z., Sencar, J., Bronzovic, M., 2009. Radioactive contamination in Croatia by phosphate fertilizer production. J. Hazard. Mater. 162, 1199–1203. https://doi.org/10.1016/j.jhazmat.2008.06.005.

Burg, A., Gavrieli, I., 2013. Groundwater contamination and water-rock interaction during leakage of industrial waste water into a carbonate aquifer in an arid zone, Israel. Procedia Earth Planet. Sci. 7, 101–104. https://doi.org/10.1016/j.proeps.2013.03.156.

Burg, A., Guttman, J., 2019. Mitigation of downstream propagation of contaminated water in a carbonate aquifer – the northeastern Negev desert, Israel. Sci. Total Environ. 654, 550–562. https://doi.org/10.1016/j.scitotenv.2018.11.103.

Burg, A., Naor, H., 2000. Well Efe13: Results Indicate Judea Group Aquifer Contamination in Rotem Area and Recommendation for Remediation, Tel Aviv, Israel (in Hebrew).

Burnett, W.C., Elzerman, A.W., 2001. Nuclide migration and the environmental radiochemistry of Florida phosphogypsum. J. Environ. Radioact. 54, 27–51. https://doi.org/10.1016/s0265-931x(00)00164-8.

Capo, R.C., Stewart, B.W., Chadwick, O.A., 1998. Strontium isotopes as tracers of ecosystem processes: theory and methods. Geoderma 82, 197–225. https://doi.org/10.1016/S0016-7061(97)00102-X.

Compton, J.S., Hodell, D.A., Garrido, J.R., Mallinson, D.J., 1993. Origin and age of phosphorite from the south-Central Florida platform: relation of phosphogenesis to sea-level fluctuations and δ13C excursions. Geochim. Cosmochim. Acta 57, 131–146. https://doi.org/10.1016/0016-7037(93)90474-B.

Cook, P.H., Herczeg, A.L., 2000. Environmental Tracers in Subsurface Hydrology. Springer Science, New York https://doi.org/10.1007/978-1-4615-4557-6.

Cotter-Howells, J., Caporn, S., 1996. Remediation of contaminated land by formation of heavy metal phosphates. Appl. Geochem. 11, 335–342. https://doi.org/10.1016/0883-2927(95)00042-9.

Gill, D., Shiloni, Y., 1995. Abundance and distribution of uranium in Senonian phosphorites, Arad basin, southern Israel. J. Afr. Earth Sci. 20, 17–28. https://doi.org/10.1016/0899-5362(95)00041-Q.

Gnandi, K., Tchangbedji, G., Killi, K., Baba, G., Abbe, K., 2006. The impact of phosphate mine tailings on the bioaccumulation of heavy metals in marine fish and crustaceans from the coastal zone of Togo. Mine Water Environ. 25, 56–62. https://doi.org/10.1007/s10230-006-0108-4.

Hamilton, S.J., Buhl, K.J., Lamothe, P.J., 2002. Selenium and other trace elements in water, sediment, aquatic plants, aquatic invertebrates, and fish from streams in southeastern Idaho near phosphate mining operations: June 2000. Final Report as part of the USGS Western U.S. Phosphate Project. U.S. Geological Survey, Columbia Environmental Research Center. https://www.cerc.usgs.gov/pubs/center/pdfDocs/91237.pdf access 8/5/22.

Harkness, J.S., Darrah, T.H., Warner, N.R., Whyte, C.J., Moore, M.T., Millot, R., Kloppmann, W., Jackson, R.B., Vengosh, A., 2017. The geochemistry of naturally occurring methane and saline groundwater in an area of unconventional shale gas development. Geochim. Cosmochim. Acta 208, 302–334. https://doi.org/10.1016/j.gca.2017.03.039.

Holtan, H., Kamp-Nielsen, L., Stuanes, A.O., 1988. Phosphorus in soil, water and sediment: an overview. In: Persson, G., Jansson, M. (Eds.), Phosphorus in Freshwater Ecosystems. Developments in Hydrobiology. 48. Springer, Dordrecht. https://doi.org/10.1007/978-94-009-3109-1_3.

Jiao, W., Chen, W., Chang, A.C., Page, A.L., 2012. Environmental risks of trace elements associated with long-term phosphate fertilizers applications: a review. Environ. Pollut. 168, 44–53. https://doi.org/10.1016/j.envpol.2012.03.052.

Jiries, A., El-Hasan, T., Al-Hweiti, M., Seiler, K.-P., 2004. Evaluation of the effluent water quality produced at phosphate mines in Central Jordan. Mine Water Environ. 23, 133–137. https://doi.org/10.1007/s10230-004-0053-z.

Khelifi, F., Mokadem, N., Liu, G., Yousaf, B., Zhou, H., Ncibi, K., Hamed, Y., 2022. Occurrence, contamination evaluation and health risks of trace metals within soil, sediments and tailings in southern Tunisia. Int. J. Environ. Sci. Technol. 19, 6127–6140. https://doi.org/10.1007/s13762-021-03531-8.

Kratz, S., Schick, J., Schnug, E., 2016. Trace elements in rock phosphates and P containing mineral and organo-mineral fertilizers sold in Germany. Sci. Total Environ. 542, 1013–1019. https://doi.org/10.1016/j.scitotenv.2015.08.046.

Li, H., Yang, Z., Dai, M., Diao, X., Dai, S., Fang, T., Dong, X., 2020. Input of cd from agriculture phosphate fertilizer application in China during 2006–2016. Sci. Total Environ. 698, 134149. https://doi.org/10.1016/j.scitotenv.2019.134149.

Mabrouk, L., Mabrouk, W., Mansour, H.B., 2020. High leaf fluctuating asymmetry in two native plants growing in heavy metal-contaminated soil: the case of metlaoui phosphate mining basin (Gafsa, Tunisia). Environ. Monit. Assess. 192, 406. https://doi.org/10.1007/s10661-020-08385-0.

Macías, F., Pérez-López, R., Cánovas, C.R., Carrero, S., Cruz-Hernandez, P., 2017. Environmental assessment and management of Phosphogypsum according to European and United States of America regulations. Procedia Earth Planet. Sci. 17, 666–669. https://doi.org/10.1016/j.proeps.2016.12.178.

Mallinson, D.J., Compton, J.S., Snyder, S.W., Hodell, D.A., 1994. Strontium isotopes and miocene sequence stratigraphy across the Northeast Florida platform. J. Sediment. Res. 64, 392–407. https://doi.org/10.1306/D4267FD2-2B26-11D7-8648000102C1865D.

McArthur, J.M., Sahami, A.R., Thirlwall, M., Hamilton, P.J., Osborn, A.O., 1990. Dating phosphogenesis with strontium isotopes. Geochim. Cosmochim. Acta 54, 1343–1351. https://doi.org/10.1016/0016-7037(90)90159-I.

McNutt, R.H., 2000. Strontium isotopes. In: Cook, P.G., Herczeg, A.L. (Eds.), Environmental Tracers in Subsurface Hydrology. Springer, Boston, MA https://doi.org/10.1007/978-1-4615-4557-6_8.

Menzel, R.G., 1968. Uranium, radium, and thorium content in phosphate rocks and their possible radiation hazard. J. Agric. Food Chem. 16, 231–234. https://doi.org/10.1021/jf60156a002.

Myers, T., 2013. Remediation scenarios for selenium contamination, Blackfoot watershed, Southeast Idaho, USA. Hydrogeol. J. 21, 655–671. https://doi.org/10.1007/s10040-013-0953-8.

Nio-Savala, A.G., Zhuang, Z., Ma, X., Fangmeier, A., Li, H., Tang, A., Liu, X., 2019. Cadmium pollution from phosphate fertilizers in arable soils and crops: an overview. Front. Agric. Sci. Eng. 6, 419–430. https://doi.org/10.15302/J-FASE-2019273.

Othman, I., Al-Masri, M.S., 2007. Impact of phosphate industry on the environment: a case study. Appl. Radiat. Isot. 65, 131–141. https://doi.org/10.1016/j.apradiso.2006.06.014.

Pérez-López, R., Nieto, J.M., López-Coto, I., Aguado, J.L., Bolívar, J.P., Santisteban, M., 2010. Dynamics of contaminants in phosphogypsum of the fertilizer industry of Huelva (SW Spain): from phosphate rock ore to the environment. Appl. Geochem. 25, 705–715. https://doi.org/10.1016/j.apgeochem.2010.02.003.

Reta, G., Dong, X., Li, Z., Su, B., Hu, X., Bo, H., Yu, D., Wan, H., Liu, J., Li, Y., Xu, G., Wang, K., Xu, S., 2018. Environmental impact of phosphate mining and beneficiation: review. Int. J. Hydrol. 2, 424–431. https://doi.org/10.15406/ijh.2018.02.00106.

Rosenthal, E., Zilberbrand, M., Livshitz, Y., 2007. The hydrochemical evolution of brackish groundwater in central and northern Sinai (Egypt) and in the western Negev (Israel). J. Hydrol. 337, 294–314. https://doi.org/10.1016/j.jhydrol.2007.01.042.

Ruhl, L.S., Dwyer, G.S., Hsu-Kim, H., Hower, J.C., Vengosh, A., 2014. Boron and strontium isotopic characterization of coal combustion residuals: validation of new environmental tracers. Environ. Sci. Technol. 48, 14790–14798. https://doi.org/10.1021/es503746v.

Rutherford, P.M., Dudas, M.J., Samek, R.A., 1994. Environmental impacts of phosphogypsum. Sci. Total Environ. 149, 1–38. https://doi.org/10.1016/0048-9697(94)90002-7.

Sabiha-Javied, T., Mehmood, M.M., Chaudhry, M., Tufail, M., Irfan, N., 2009. Heavy metal pollution from phosphate rock used for the production of fertilizer in Pakistan. Microchem. J. 91, 94–99. https://doi.org/10.1016/j.microc.2008.08.009.

Sattouf, M., 2007. Identifying the origin of rock phosphates and phosphorous fertilisers using isotope ratio techniques and heavy metal patterns. FAL Agricultural Research. https://d-nb.info/996740074/34.

Sattouf, M., Kratz, S., Diemer, K., Rienitz, O., Fleckenstein, J., Schiel, D., Schnug, E., 2007. Identifying the origin of rock phosphates and phosphorus fertilizers through high-precision measurement of the strontium isotopes 87Sr and 86Sr. Landbauforschung Völkenrode 57, 1–11. https://literatur.thuenen.de/digbib_extern/bitv/dk038104.pdf.

Sattouf, M., Kratz, S., Diemer, K., Fleckenstein, J., Rienitz, O., Schiel, D., Schnug, E., 2008. Significance of uranium and strontium isotope ratios for retracing the fate of uranium during the processing of phosphate fertilizers from rock phosphorites. In: De Kok, L., Schnug, E. (Eds.), Loads and Fate of Fertilizer Derived Uranium. Backhuys Publishers, Leiden, the Netherlands , pp. 191–202. https://research.rug.nl/en/publications/loads-and-fate-of-fertilizer-derived-uranium.

Schnug, E., Haneklaus, N., 2015. Uranium in phosphate fertilizers – review and outlook. In: Merkel, B.J., Arab, A. (Eds.), Uranium – Past and Future Challenges. Springer, Freiberg, Germany.

Shang, D., Geissler, B., Mew, M., Satalkina, L., Zenk, L., Tulsidas, H., Barker, L., El-Yahyaoui, A., Hussein, A., Taha, M., Zheng, Y., Wang, M., Yao, Y., Liu, X., Deng, H., Zhong, J., Li, Z., Steiner, G., Bertau, M., Haneklaus, N., 2021. Unconventional uranium in China's phosphate rock: review and outlook. Renew. Sust. Energ. Rev. 140, 110740. https://doi.org/10.1016/j.rser.2021.110740.

Silva, E.F.d., Mlayah, A., Gomes, C., Noronha, F., Charef, A., Sequeira, C., Esteves, V., Marques, A.R.F., 2010. Heavy elements in the phosphorite from Kalaat Khasba mine (North-western Tunisia): potential implications on the environment and human health. Journal of Hazardous Materials 182, 232–245. https://doi.org/10.1016/j.jhazmat.2010.06.020.

Soudry, D., 1992. Primary bedded phosphorites in the Campanian Mishash Formation, Negev, southern Israel. Sediment. Geol. 80, 77–88. https://doi.org/10.1016/0037-0738(92)90033-N.

Soudry, D., Glenn, C.R., Nathan, Y., Segal, I., VonderHaar, D., 2006. Evolution of tethyan phosphogenesis along the northern edges of the Arabian-African shield during the cretaceous-eocene as deduced from temporal variations of Ca and Nd isotopes and rates of P accumulation. Earth Sci. Rev. 78, 27–57. https://doi.org/10.1016/j.earscirev.2006.03.005.

Soudry, D., Nathan, Y., Ehrlich, S., 2013. Geochemical diagenetic trends during phosphorite formation – economic implications: the case of the Negev Campanian phosphorites, southern Israel. Sedimentology 60, 800–819. https://doi.org/10.1111/j.1365-3091.2012.01361.x.

Stein, M., Starinsky, A., Katz, A., Goldstein, S.L., Machlus, M., Schramm, A., 1997. Strontium isotopic, chemical, and sedimentological evidence for the evolution of Lake Lisan and the Dead Sea. Geochim. Cosmochim. Acta 61, 3975–3992. https://doi.org/10.1016/S0016-7037(97)00191-9.

Stille, P., Riggs, S., Clauer, N., Ames, D., Crowson, R., Snyder, S., 1994. Sr and nd isotopic analysis of phosphorite sedimentation through one Miocene high-frequency depositional cycle on the North Carolina continental shelf. Mar. Geol. 117, 253–273. https://doi.org/10.1016/0025-3227(94)90019-1.

Sun, Y., Amelung, W., Wu, B., Haneklaus, S., Maekawa, M., Lücke, A., Schnug, E., Bol, R., 2020. 'Co-evolution' of uranium concentration and oxygen stable isotope in phosphate rocks. Appl. Geochem. 114, 104476. https://doi.org/10.1016/j.apgeochem.2019.104476.

Taha, Y., Elghali, A., Hakkou, R., Benzaazoua, M., 2021. Towards zero solid waste in the sedimentary phosphate industry: challenges and opportunities. Minerals 11, 1250. https://doi.org/10.3390/min11111250.

Vengosh, A., Rosenthal, E., 1994. Saline groundwater in Israel: its bearing on the water crisis in the country. J. Hydrol. 156, 389–430. https://doi.org/10.1016/0022-1694(94)90087-6.

Vengosh, A., Hening, S., Ganor, J., Mayer, B., Weyhenmeyer, C.E., Bullen, T.D., Paytan, A., 2007. New isotopic evidence for the origin of groundwater from the Nubian sandstone aquifer in the Negev, Israel. Appl. Geochem. 22, 1052–1073. https://doi.org/10.1016/j.apgeochem.2007.01.005.

Vengosh, A., Coyte, R., Karr, J., Harkness, J.S., Kondash, A.J., Ruhl, L.S., Merola, R.B., Dywer, G.S., 2016. Origin of hexavalent chromium in drinking water Wells from the Piedmont aquifers of North Carolina. Environ. Sci. Technol. Lett. 3, 409–414. https://doi.org/10.1021/acs.estlett.6b00342.

Vengosh, A., Cowan, E.A., Coyte, R.M., Kondash, A.J., Wang, Z., Brandt, J.E., Dwyer, G., 2019. Evidence for unmonitored coal ash spills in Sutton Lake, North Carolina: implications for contamination of lake ecosystems. Sci. Total Environ. 686, 1090–1103. https://doi.org/10.1016/j.scitotenv.2019.05.188.

Vengosh, A., Coyte, R.M., Podgorski, J., Johnson, T.M., 2022. A critical review on the occurrence and distribution of the uranium- and thorium-decay nuclides and their effect on the quality of groundwater. Sci. Total Environ. 808, 151914. https://doi.org/10.1016/j.scitotenv.2021.151914.

Warner, N.R., Darrah, T.H., Jackson, R.B., Millot, R., Kloppmann, W., Vengosh, A., 2014. New tracers identify hydraulic fracturing fluids and accidental releases from oil and gas operations. Environ. Sci. Technol. 48, 12552–12560. https://doi.org/10.1021/es5032135.

Wilde, F.D., 2008. Chapter A6.0, General Information and Guidelines: U.S. Geological Survey Techniques of Water-Resources Investigations. U.S. Geological Survey. https://doi.org/10.3133/twri09A6.0.

World Bank Group, 2007. Environmental, Health and Safety Guidelines for Phosphate Fertilizer Manufacturing. https://documents1.worldbank.org/curated/en/549491489583284931/pdf/113496-WP-ENGLISH-Phosphate-Fertilizer-Plants-PUBLIC.pdf (access 7/2/2022).

Zhuang, P., McBride, M.B., 2013. Changes during a century in trace element and macronutrient concentrations of an agricultural soil. Soil Sci. 178. https://doi.org/10.1097/SS.0b013e318290b8fa.